

Molecular Motion in Cured Epoxy Resin Filled with Mica Flakes

K. IISAKA and K. SHIBAYAMA, *Manufacturing Development Laboratory, Mitsubishi Electric Corporation, Amagasaki, Hyogo, Japan*

Synopsis

Molecular motion in cured epoxy resin filled with mica flakes was investigated by dynamic mechanical and broad-line nuclear magnetic resonance measurements. Temperature dependences of dynamic modulus and $\tan\delta$ were determined at 10 Hz for samples containing various amounts of filler. A primary dispersion temperature, T_{α} , corresponding to the glass transition, shifts to higher temperature with increasing filler volume fraction V_f . The magnitudes of the slope parameters H_r (representing storage modulus E' data above T_g) decreased with increasing V_f , but H_g (representing E' data below T_g) remained nearly constant over the whole loading range studied here. NMR line shapes were observed over the temperature range from room temperature to about 200°C for unfilled and filled samples. Each sample showed a distorted line shape in the transition region where major narrowing occurs. The distorted line shape was decomposed into both broad and narrow components by Gaussian analysis. The temperature range where both components can be obtained becomes broader with increasing filler content. The possibility is set forth that the filler immobilizes the chain segments and causes a different distribution of local mobility around the junction point.

INTRODUCTION

Increases in the glass transition temperature (T_g) were observed in polyisobutylene filled with glass beads,¹ phenoxy resin filled with clay,² styrene-methyl methacrylate copolymer filled with silica,³ cured epoxy resin filled with TiO_2 ,⁴ and cured epoxy resin filled with quartz⁵ by DTA and dynamic mechanical measurements. The increase in T_g apparently depends on volume fraction of filler and could be due to the immobilization of polymer segments near the filler surface. We have reported⁶ that as determined by the dynamic mechanical investigation of cured epoxy resin filled with mica flake, the dynamic modulus of the filled resin is extraordinarily high, comparing with that of other usual fillers. It is of interest to investigate molecular motion in mica-filled resin.

NMR is a useful tool for the study of filled systems because the NMR measurement is affected by short-range molecular motion. The NMR studies in filled epoxy resin have been done on uncured systems of bisphenol A-epichlorohydrin epoxy resin filled with fine silica⁷ and epoxy oligomer filled with thermoplastic polymer.⁸ Until recently, there has been little investigation in cured epoxy resin with filler.

Results of NMR studies of molecular motion in solid polymers so far reported have been discussed mainly in terms of linewidth, second moment, and relaxation times. Line shape has been subjected to arguments only when it has clearly separable components as in the cases of partially crystalline polymers and polymers having side chains, such as poly(methyl methacrylate). It is assumed here that even when the line shape has no clearly separable components, the

shape can be characteristic of the nature of a polymeric system through a distortion or a certain change in the line-shape function in the transition region and that the line shape of a filled system is different from that of the base polymer. In the present NMR study, special attention is paid to line shape in the transition region. Here, we have investigated the effect of filler on the segmental motion in cured epoxy resin by dynamic mechanical and NMR measurements.

EXPERIMENTAL

Small muscovite mica flake about 1 μm thick and 100 μm wide was used as the filler. Mica flake was obtained by crushing mechanically a reconstituted mica paper supplied by the 3M Company and sifting out the 28–40 mesh portion used. Mica flakes were dried for 24 hr at 120°C before use.

Unfilled batches of epoxy were made with a composition ratio for Epikote 828 (Shell Chemical Co.):methyl nadic anhydride:caprylic acid zinc salt of 100:90:2 and were cast into sheet specimens between two glass plates. Preparation of the composites were accomplished by mixing various amounts of filler and resin (with the same composition ratio as the unfilled one) in a mortar and casting into sheet specimens between two glass plates. These samples were cured at 150°C for 16 hr. Table I lists the filler volume fraction in the composites determined from the residue by burning out the specimen at 500°C for 3 hr in air.

Measurements of dynamic mechanical properties were carried out over the temperature range from 20° to about 200°C at 10 Hz by a viscoelastic spectrometer (Iwamoto Seisakusho Co., Kyoto, Japan). The spectrometer in the NMR study was the usual broad-line NMR instrument operating at 17 MHz with the signal detector of a Pound-Watkins-type marginal oscillator. Homogeneity of magnetic field over the sample volume was of the order of 100 mG. Line-shape measurements were accomplished at a low enough rf field so as not to saturate the absorption line over the temperature range from room temperature to about 200°C. The modulation amplitude was chosen to be less than a quarter of the linewidth.

RESULTS AND DISCUSSION

Figure 1 shows the temperature dependence of the storage modulus E' and $\tan \delta$ for each sample. The increase in storage modulus with loading is outstanding over the whole temperature range, as reported in the previous paper.⁶ Mechanical loss peaks were observed at temperatures ranging from about 130°–150°C. These peaks are associated with the microbrownian motion of

TABLE I
Composition

Sample	Composition, vol-%	
	Resin	Mica
R	100	0
RM1	93.8	6.2
RM2	83.6	16.4
RM3	71.4	28.6
RM4	51.1	48.9

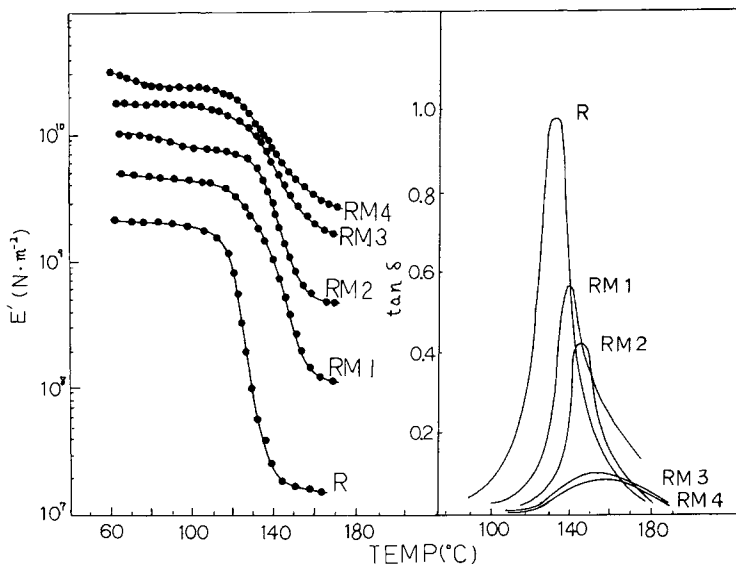


Fig. 1. Temperature dependence of storage modulus E' and $\tan \delta$.

matrix chain segments, corresponding to the glass transition. They shifted to a higher temperature with increase in filler content. Figure 2 shows the shift in the temperature of $\tan \delta$ maximum, ΔT_α , versus filler volume fraction V_f . T_α rapidly increases in the lower loading region. The $\tan \delta$ curves had single peaks and became broader with increase in filler content, but no secondary peak was apparent in the temperature region of the primary dispersion.

The parameter H representing the steepness of frequency dispersion can be obtained from the temperature dependence of the modulus by eq. (1)⁴:

$$\log \left(\frac{E'}{E_2'} \right) / \log \left(\frac{E_1'}{E_2'} \right) = \frac{1}{2} \left\{ 1 + \operatorname{erf} H \left[\left(\frac{1}{T} \right) - \left(\frac{1}{T_0} \right) \right] \right\} \quad (1)$$

where E_1' and E_2' are the upper and lower plateau values of the dynamic modulus, T_0 is the temperature at which $E' = (E_1' \cdot E_2')^{1/2}$, and erf is the error function. A plot of the left-hand side of eq. (1) versus $(1/T) - (1/T_0)$ on normal probability paper should yield a straight line from the slope of which H can be calculated.⁹

In a filled system, a decrease in the slope of $\log E'$ versus $\log t$ always occurs

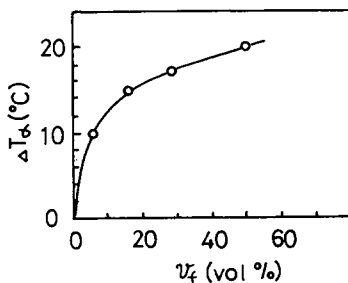


Fig. 2. Plot of ΔT_α vs v_f .

because the ratio of the matrix modulus to the filler modulus is much smaller at the rubbery end of the transition than it is at the glassy end. To eliminate such an influence, we have divided the modulus data for the composites by an appropriate correction factor. Here, in order to evaluate a change in H qualitatively, we have adopted the correction factor computed from Kerner's equation, though the latter is for spherical fillers. Plots of modulus data according to eq. (1) yielded curves represented by two straight lines intersecting at or near $(1/T) - (1/T_0) = 0$. The data obtained above and below the transition temperature for the different filler contents are described by the slope parameters H_r and H_g in Figure 3. The H_r value decreased at a greater rate at lower loading range, while the H_g value is nearly constant over the whole loading range studied here. The lower values of H_r for the filled polymers suggested the possibility of a different distribution of local mobility around the junction point as a result of filler presence.

It is the main purpose of this paper to obtain evidence which supports the dynamic mechanical results in the transition region by the NMR method where the internal motion in the solid state can be observed more directly. NMR linewidth was about 5.0 G at room temperature, irrespective of the kind of sample. The linewidth decreased rapidly in the transition temperature region. Figure 4 shows the temperature dependence of the second moment for the samples R, RM3, and RM4. The transition temperature shifted to a higher temperature with increase in filler content. Figure 5 shows examples of one half of the differential absorption lines observed in this study at each temperature of the glassy and the transition region for R and RM4. Certain distortions can be seen apparently in line shapes in the middle of the transition region. Two general types of line shapes so far discussed are the Gaussian and the Lorentzian distribution of intensity around the center of resonance, corresponding with the rigid state in which the direct dipole-dipole interaction prevails and the mobile state in which the internal motion occurs at a sufficiently low frequency, respectively.^{10,11} Differential absorption lines can be expressed as eqs. (2) and (3) for the Gaussian and the Lorentzian distribution, respectively:

$$I(u) = -2ABu \exp(-Bu^2) \quad (2)$$

$$I(u) = -2ABu(1 + Bu^2)^{-2} \quad (3)$$

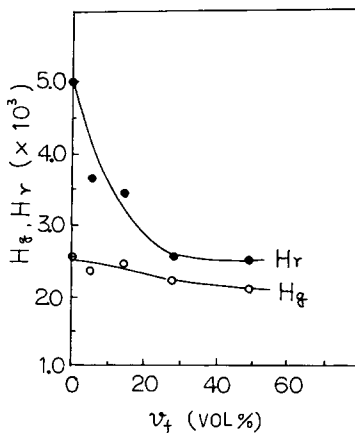


Fig. 3. Plot of H_g and H_r vs v_f .

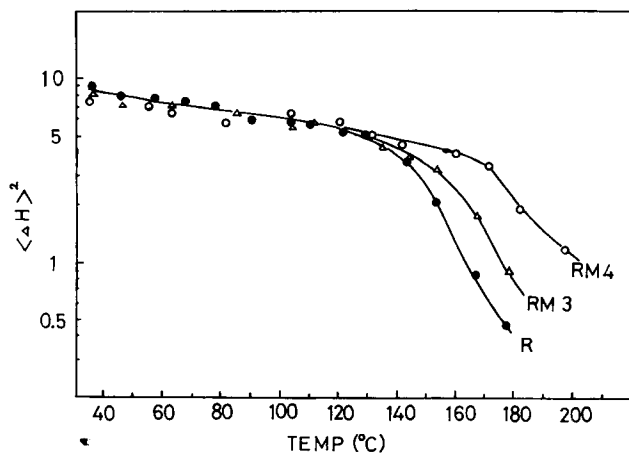


Fig. 4. Temperature dependence of second moment.

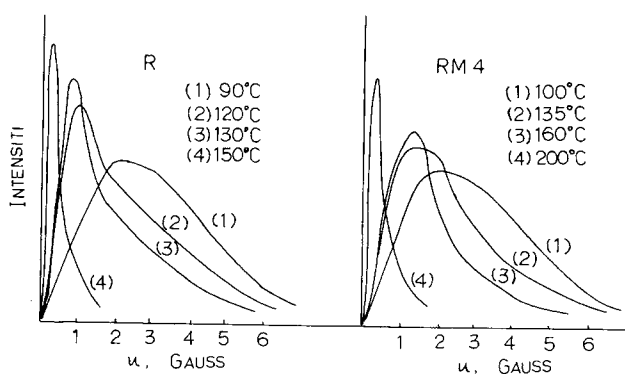


Fig. 5. Variation of line shapes with temperature through the transition region for samples R and RM4.

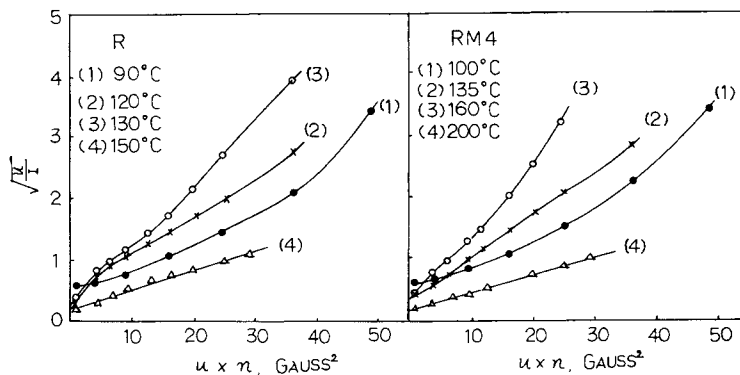


Fig. 6. Lorentzian plots of the observed line shapes for samples R and RM4.

where $I(u)$ is the intensity at a sweep field u measured from the center of the resonance, and A and B are constants. Straight lines are to be expected when $\log(I/u)$ is plotted versus u^2 in the case of the Gaussian distribution and when $\sqrt{u/I}$ is plotted versus u^2 in the case of the Lorentzian distribution. Observed absorption lines are converted to the plot by eqs. (2) and (3), as shown in Figures

6 and 7. It is clear from the figures that the line shapes for the unfilled and filled samples are approximately Gaussian in the case of the glassy state at lower temperature and Lorentzian in the case of the completely narrowed line at higher temperature, respectively, in conformity with the general discussion. Difficulties remain in the transition region where single straight lines are not seen in the Gaussian plot, and irregular curvatures are given in the Lorentzian plot. In the former case, the plot yields a straight line for larger values of u though ambiguities are associated with the line for smaller values of u . These results show that the line shape in the transition region can be approximated by a superposition of one Gaussian curve having a larger width and a certain unknown curve having a smaller width.

Here, we have tried to decompose observed absorption lines into two lines. One of them is the Gaussian line of larger width derived by the Gaussian plot illustrated in Figure 7, and the other one is the narrow line derived by subtracting the Gaussian line from the observed absorption line. Examples of these decompositions are shown in Figure 8. Here, the line width seems to be inaccurate due to the fact that the linewidth of the narrow component may be affected, at least to some degree, by the broad component. From such analysis of the line shapes in the transition region, the temperature where the broad component begins to decrease shifts to a higher temperature with increasing V_f , and the temperature range where both components can be derived becomes broader, changing from about 48° to 88°C in going from R to RM4, as indicated in Table II.

Both a narrow and a broad line were reported⁷ to be present in the transition region between 300° and 330°K in an uncured epoxy resin, though the molecular mechanisms were not discussed. From Figure 4, at about 120°C, the observed second moment $\langle \Delta H \rangle^2$ is ca. 6.0 gauss,² and hence other groups as well as the methyl groups must be in molecular motion.⁷ In the present study, a molecular chain is assumed to be composed of one portion which is more restricted in its motion near the polymer-filler junction point and another one which is far from the junction point and mobile. Each segmental motion of both portions in the unfilled sample would be restricted, but to different degrees, by the filler surface. The appearance and growth of the broad component with decreasing temperatures can be considered to correspond to the onset and completion of the freez-

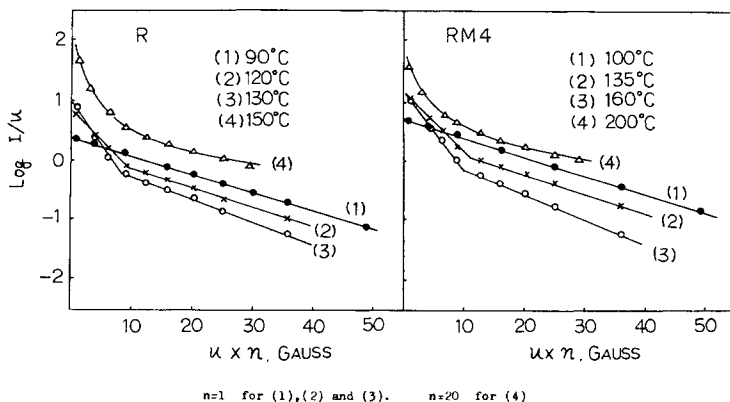


Fig. 7. Gaussian plots of observed line shapes for samples R and RM4; $n = 1$ for (1), (2), and (3); $n = 20$ for (4).

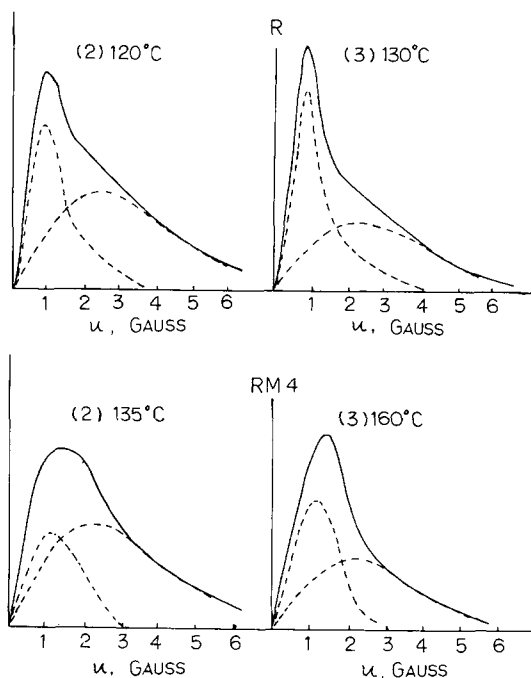


Fig. 8. Analysis of distorted line shapes by Gaussian curves. Solid and dashed curves represent observed and decomposed line, respectively.

TABLE II
Line Shapes in The Transition Region Characterized by Gaussian Analysis

	Sample		
	R	RM3	RM4
Temperature where the narrow component begins to appear, °C	90	98	108
Temperature range where both components can be derived, °C	45-50	60-65	85-90

ing-in process in segmental motion. The present NMR results, namely, that the broad component in the transition region persists to higher temperatures with an increase of filler content, seem to reflect on the presence of a distribution in segmental mobilities.

It is well known¹² that the glass transition temperature of a polymer increases with increasing crosslinking density ρ . And the increase in ρ decreases regularly the parameter h , which represents the steepness of the frequency dispersion.¹³ In filled network polymers, the segmental adsorption on the filler surface would be regarded as an additional network junction over that of unfilled network polymers. It is concluded that incorporation of the filler into the polymer makes segmental mobilities of a chain more inhomogeneous compared with those of the unfilled network polymer.

References

1. R. F. Landel, *Trans. Soc. Rheol.*, **2**, 53 (1958).
2. D. H. Droste and T. A. DiBenedetto, *J. Appl. Polym. Sci.*, **13**, 2149 (1969).

3. Y. S. Lipatov and F. G. Fabulyak, *J. Appl. Polym. Sci.*, **16**, 2131 (1972).
4. I. Galperin, *J. Appl. Polym. Sci.*, **11**, 1475 (1969).
5. Y. S. Lipatov, V. F. Babich, and V. F. Rosovizky, *J. Appl. Polym. Sci.*, **18**, 1213 (1974).
6. K. Iisaka and K. Shibayama, *J. Appl. Polym. Sci.*, **20**, 813 (1976).
7. C. C. Monks and B. Ellis, *J. Polym. Sci. A-2*, **8**, 2203 (1970).
8. Y. S. Lipatov and F. G. Fabulyak, *Vysokomol. Soedin.*, **A15** (No. 6), 1272 (1973).
9. P. Theocaris, *J. Appl. Polym. Sci.*, **8**, 399 (1964).
10. G. E. Pake and E. M. Purcell, *Phys. Rev.*, **79**, 1134 (1948).
11. R. Kubo and K. Tomita, *J. Phys. Soc., Jpn.*, **9**, 888 (1945).
12. T. Fox and P. Flory, *J. Appl. Phys.*, **21**, 581 (1950).
13. K. Shibayama and Y. Suzuki, *J. Polym. Sci. A*, **3**, 2637 (1965).

Received June 11, 1976

Revised May 9, 1977